Properties of Excitatory Synaptic Connections Mediated by the Corpus Callosum in the Developing Rat Neocortex

SANJAY S. KUMAR AND JOHN R. HUGUENARD
Department of Neurology and Neurological Sciences, Stanford University Medical Center, Stanford, California 94305-5122

Received 26 April 2001; accepted in final form 14 August 2001

Kumar, Sanjay S. and John R. Huguenard. Properties of excitatory synaptic connections mediated by the corpus callosum in the developing rat neocortex. *J Neurophysiol* 86: 2973–2985, 2001. Despite the major role of excitatory cortico-cortical connections in mediating neocortical activities, little is known about these synapses at the cellular level. Here we have characterized the synaptic properties of long-range excitatory-to-excitatory contacts between visually identified layer V pyramidal neurons of agranular frontal cortex in callosally connected neocortical slices from *postnatal day 13* to *21* (*P13–21*) rats. Midline stimulation of the corpus callosum with a minimal stimulation paradigm evoked inward excitatory postsynaptic currents (EPSCs) with an averaged peak amplitude of 56.5 ± 5 pA under conditions of whole cell voltage clamp at −70 mV. EPSCs had fixed latencies from stimulus onset and could follow stimulus trains (1–20 Hz) without changes in kinetic properties. Bath application of 2,3-dihydro-6-nitro-7-sulfamoyl-benzo-(F)quinoxaline (NBQX) abolished these responses completely, indicating that they were mediated by α-amino-3-hydroxy-5-methyl-4-isoxazolepropionic acid (AMPA) receptors (AMPARs). Evoked responses were isolated in picrotoxin to yield purely excitatory PSCs, and a low concentration of NBQX (0.1 μM) was used to partially block AMPARs and prevent epileptiform activity in the tissue. Depolarization of the recorded pyramidal neurons revealed a late, slowly decaying component that reversed at ~0 mV and was blocked by D-2-amino-5-phosphonovaleric acid. Thus AMPA and *N*-methyl-D-aspartate receptors (NMDARs) coexist at callosal synapses and are likely to be activated monosynaptically. The peak amplitudes and decay time constants for EPSCs evoked using minimal stimulation (±40 mV) were similar to spontaneously occurring sEPSCs. Typical conductances associated with AMPA and NMDAR-mediated components, deduced from their respective current-voltage (*I-V*) relationships, were 525 ± 168 and 966 ± 281 pS, respectively. AMPAR-mediated responses showed age-dependent changes in the rectification properties of their *I-V* relationships. While *I-V*s from animals *>P15* were linear, those in the younger (*<P16*) age group were inwardly rectifying. Although Ca^{2+} permeability in AMPARs can be correlated with inward rectification, outside-out somatic patches from younger animals were characterized by Ca^{2+}-impermeable receptors, suggesting that somatic receptors might be functionally different from those located at synapses. While the biophysical properties of AMPAR components of callosally-evoked EPSCs were similar to those evoked by stimulation of local excitatory connections, the NMDA component displayed input-specific differences. NMDAR-mediated responses for local inputs were activated at more hyperpolarized holding potentials in contrast with those evoked by callosal stimulation. Paired stimuli used to assay presynaptic release properties showed paired-pulse depression (PPD) in animals *<P16*, which converted to facilitation (PPF) in older animals, suggesting a developmental transition from low probability of transmitter release to high P_r at these synapses and/or alterations in the properties of the underlying postsynaptic receptors. Physiologic properties of neocortical e-e connections are thus input specific and subject to developmental changes in their postsynaptic receptors.

INTRODUCTION

Eighty-five percent of synapses within the mammalian neocortex are excitatory with a large majority originating from cortical neurons; 85% of the synapses made by excitatory neurons are onto other excitatory neurons (Braitenberg and Schüz 1991; Douglas et al. 1995; Kisvarday et al. 1986; McGuire et al. 1984). Despite these numbers, which suggest a strong contribution of excitatory cortico-cortical synapses to the response properties of individual neurons and overall excitability of the neocortex, it has been difficult to characterize the physiological properties and receptor composition of individual excitatory-to-excitatory (e-e) synapses. The complexity of the excitatory circuitry together with the difficulty of isolating purely excitatory monosynaptic responses without causing tissue hyperexcitability, as occurs for example with the blockade of GABA-ergic transmission, are factors that have hindered progress on this front (Avoli et al. 1997; Sutor and Luhmann 1998). Furthermore, the probability of finding a synaptic connection in dual recordings from pairs of adjacent pyramids can be also surprisingly low (Markram et al. 1997).

The corpus callosum is the principal commissural pathway in the forebrain linking the two cerebral hemispheres. The cells of origin of neocortical callosal projections are almost entirely pyramidal cells, located mainly in layers II/III and V, that terminate exclusively with excitatory asymmetric synapses on spines of pyramidal neurons in homo- and heterotopic regions of the contralateral cortex (Akers and Killackey 1978; Jacobson 1965; Jacobson and Trojanowski 1974; Pandya and Seltzer 1986; Wise and Jones 1976). Callosal projections are amenable to reliable electrical stimulation (Vogt and Gorman 1982) and, as they are purely excitatory, lend themselves well to the study of e-e synapses (Aram and Lodge 1988) and intracortical excitation. Furthermore, the callosum is considered a primary substrate for intrahemispheric spread of discharges in generalized epileptic seizures (Gazzaniga et al. 1975; Reeves and O'Leary 1985). Clinical studies have shown that ablation of

Address reprint requests to J. R. Huguenard (E-mail: John.Huguenard@Stanford.EDU).

The costs of publication of this article were defrayed in part by the payment of page charges. The article must therefore be hereby marked "*advertisement*" in accordance with 18 U.S.C. Section 1734 solely to indicate this fact.

this pathway (callosotomy) can eliminate seizure activity or decrease its severity and frequency, suggesting that intracortical excitation can initiate and/or perpetuate epileptiform activity. Excitatory cortico-cortical projections may play a crucial role in determining the strength and extent of its generalization, especially during critical periods in early maturation when neocortical tissue is vulnerable to epileptiform activity (Luhmann and Prince 1990; Moshe et al. 1983; Swann et al. 1993).

Our aim in this study was to assay the viability of using the corpus callosum as a model system for the study of intracortical excitability by *1*) investigating the receptor composition of the callosal synapse; *2*) characterizing the voltage dependence of the pharmacologically isolated components of excitatory postsynaptic currents (EPSCs) evoked by minimal stimulation of the callosum; *3*) determining whether the kinetic properties of spontaneous and evoked EPSCs recorded in these neurons can reveal differences in function of the underlying receptor populations at callosal and noncallosal synapses; and *4*) noting changes in the physiologic properties of these receptors as a function age in the range considered.

Characterization of synaptic currents mediated by these receptors first required the isolation of purely excitatory monosynaptic responses with minimal contribution from polysynaptic events such as those arising from feed-forward excitation. Toward this end, a minimal stimulation paradigm was used in conjunction with a pharmacologically controlled blockade of inhibition. Callosally evoked responses were compared with EPSCs evoked during stimulation of local excitatory circuitry in the vicinity of the recorded neuron to determine differences in the biophysical properties of the underlying receptor subtypes and the input specificity of their responses. Our results indicate that minimal stimulation of the callosum can evoke an *N*-methyl-D-aspartate (NMDA) receptor–mediated monosynaptic EPSC in layer V pyramidal neurons in addition to the non-NMDA or α-amino-3-hydroxy-5-methyl-4-isoxazolepropionic acid (AMPA) component, reported in previous studies (Kawaguchi 1992; Vogt and Gorman 1982). Interestingly, however, while the functional properties of AMPARs were common among synaptic inputs onto the neuron, the NMDARs displayed input-specific differences in their activation. To characterize the callosal synapse further, we also ascertained, using paired stimuli, its presynaptic release properties. Postsynaptic changes in receptor function were assayed in conjunction using evoked and spontaneous EPSC data. Portions of this work have been presented earlier in abstract form (Kumar and Huguenard 1999).

METHODS

In vitro slice preparation

Briefly, rat pups (Sprague-Dawley) were anesthetized using 50 mg/kg pentobarbital sodium, administered intraperitoneally, and decapitated, and the brains were rapidly removed and transferred to a chilled (4°C) low-Ca^{2+}, low-Na^{+} slicing solution containing (in mM) 234 sucrose, 11 glucose, 24 $NaHCO_3$, 2.5 KCl, 1.25 NaH_2PO_4, 10 $MgSO_4$, and 0.5 $CaCl_2$ equilibrated with a 95:5% mixture of O_2 and CO_2. Brains were subsequently blocked, and coronal slices, 300 μm thick, were prepared on a vibratome (blade angle, 18°) and incubated at 32°C in oxygenated artificial cerebrospinal fluid (ACSF, in mM: 126 NaCl, 26 $NaHCO_3$, 2.5 KCl, 1.25 NaH_2PO_4, 2 $MgCl_2$, 2 $CaCl_2$, and 10 glucose; pH 7.4) for 1 h before recordings began.

Electrophysiology

Whole cell patch-clamp recordings were made from layer V pyramidal neurons using a visualized infrared setup such that neuron morphology and location within the various cortical lamina could be identified. Recording electrodes (1.2- to 2-μm tip diameters, 3–6 MΩ) contained (in mM) 120 cesium gluconate, 1 $MgCl_2$, 1 $CaCl_2$, 11 KCl, 10 HEPES, 2 NaATP, 0.3 NaGTP, and 11 EGTA (pH 7.3 corrected with Cs-OH, 290 mOsm). QX-314 (1 mM) was also included in the patch solution to block postsynaptic action potential–mediated events. Membrane potentials were corrected for a liquid junction potential of +10 mV for cesium gluconate in all experiments. Drugs and chemicals were applied through the perfusate that was continuously oxygenated with 95% O_2-5% CO_2. The exchange time for the recording chamber was ~3 min, and all recordings were obtained at 32 ± 1°C. Concentric bipolar electrodes (CB-XRC75, Frederick Haer) with 75-μm tip diameters were positioned on the callosal tract and/or intracortically in close proximity to the recorded neuron (Fig. 1*A*), and constant-current pulses 50–300 μs in duration and 100–500 μA in amplitude were applied at low frequencies (0.1–0.3 Hz). Minimal stimulation parameters were determined by increasing current strength until an all-or-none postsynaptic response could be evoked while holding the cell at −70 mV and were held constant just above threshold (1.2*T*) throughout the remainder of the experiment. EPSCs were recorded with an Axopatch 1D (Axon Instruments), filtered at (0.5–1 kHz), and digitized at 10 kHz with PClamp (Axon Instruments) software. Data were concurrently digitized (44 kHz) using a Neurocorder DR-484 (Neuro Data Instruments) and stored on VHS videotapes. Series resistance was monitored continuously, and experiments in which it changed by more than 20% were excluded from further analysis. No series resistance compensation was used in the experiments. Spontaneous synaptic responses were analyzed separately using Mini Analysis (Synaptosoft) and homemade software (Metatape and Detector). The threshold for detecting sEPSCs was set at 2.5–3 times root-mean-square (RMS) noise level. Time constants for PSCs were obtained from single exponential fits of averaged records using Clampfit (Axon Instruments), and traces shown in the figures are averages of at least 10 consecutive responses. All values are expressed as means ± SE, and statistical differences were measured with the Student's *t*-test or the Kolmogorov-Smirnov (K-S) test, unless indicated otherwise. The following were bath applied separately or in combination as required for specific protocols: D(−)-2-amino-5-phosphonopentanoic acid (D-APV), 2,3-dihydro-6-nitro-7-sulfamoyl-benzo(F)quinoxaline [NBQX; concentrated stock made up in dimethylsulphoxide (DMSO) <0.1% final concentration], and picrotoxin (all from RBI/Sigma).

Outside-out patches were obtained from layer V pyramidal neurons, identified visually based on their characteristic morphology using a ×60 objective. Neurons were approached at their somas with a patch pipette under positive pressure (40 millibars). Patch electrodes had resistances in the range of 2–5 MΩ when filled with an internal solution containing (in mM) 140 CsCl, 10 EGTA, 2 $MgCl_2$, 2 NaATP, 10 HEPES (pH 7.3 corrected with Cs-OH, 290 mOsm). Following the release of positive pressure and formation of a gigaohm seal, the patch pipette was gently pulled away from the soma after break-in (whole cell configuration) and lifted above the surface of the slice into the bath with the aid of a motorized (TS products, Post Falls, ID) micromanipulator. This procedure resulted in the formation of a stable outside-out patch (Hamill et al. 1981). The patch pipette was subsequently displaced rapidly to a predetermined location in the recording chamber superfused continuously with oxygenated ACSF, and rapid application of the agonist (glutamate) was achieved using a method similar to Jonas and Sakmann (1992) and Colquhoun et al. (1992). Briefly, an application pipette made from a theta (θ) glass capillary (Sutter Instruments, Novato, CA; 1.5 mm OD; tip diameter: 150–200 μm; wall thickness: 0.3 mm; septum thickness: 0.16 mm) was mounted directly onto a piezoelectric device and positioned in the

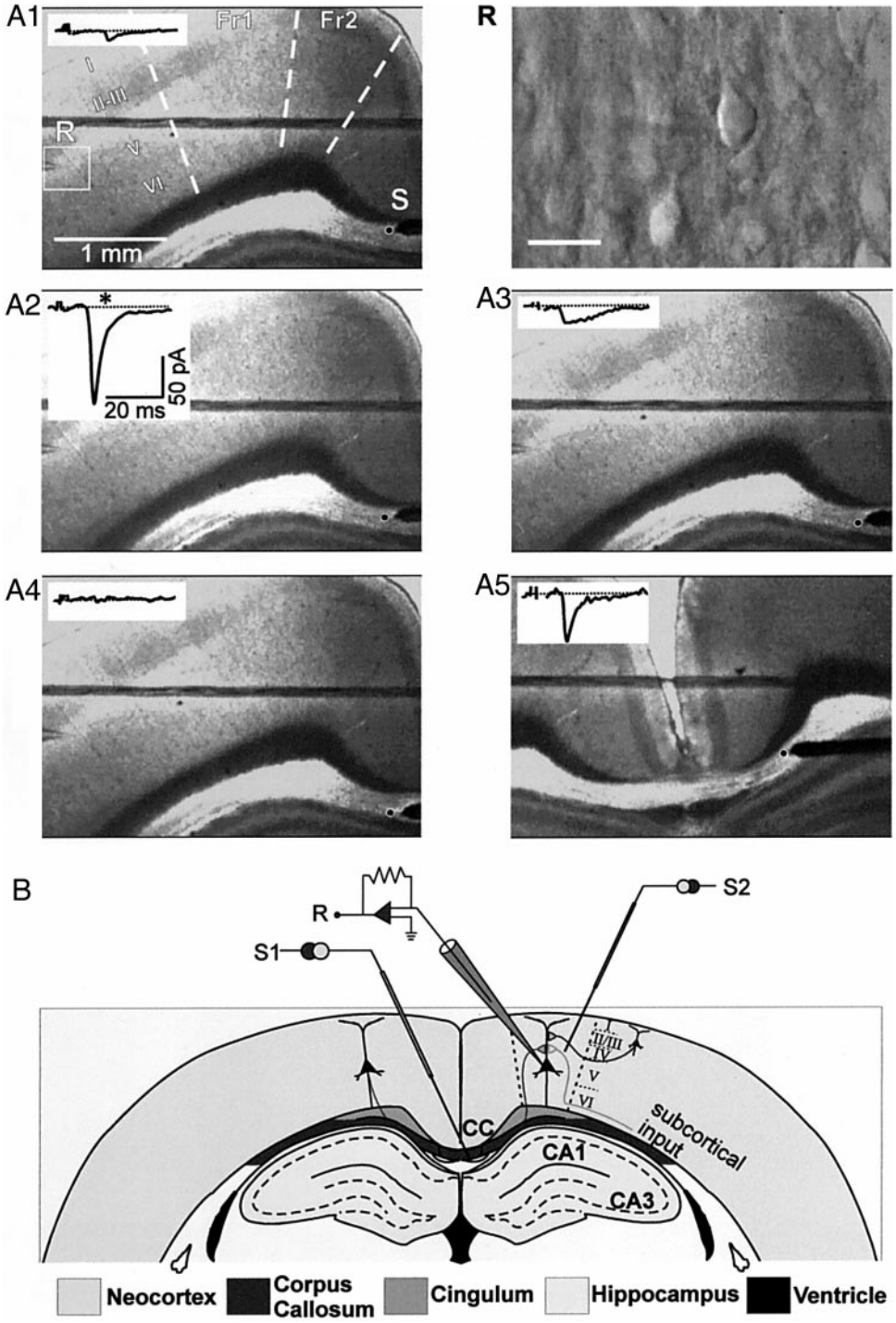

FIG. 1. The callosal slice preparation and schematic. *A1–A5*: low-powered images of a coronal cortical section, obtained with a ×10 objective, depicting placement of a bipolar stimulating electrode (S in *A1*) at different locations (●) along the dorsal-ventral extent of the callosum. The corresponding whole cell responses of a layer V pyramidal neuron (R in *A1*) evoked by stimulation of the callosum at these locations are shown as *insets.* Traces are averages of ≥10 responses evoked at the holding potential of −70 mV, and stimulus intensity was constant throughout. Patch pipette in *A1* is visible during whole cell recording from pyramidal neuron on the right (R, scale bar is 40 μm). Note that responses were especially robust at one near-midline location (* in *A2*). Postsynaptic currents (PSCs) with longer latency and similar kinetic properties could also be evoked from the contralateral hemisphere (*A5*). Typical recording region was usually closer to midline in the frontal-cortex areas 1 and 2 (Fr1 and Fr2, *A1*). *B*: schematic of the slice preparation showing typical placement of the stimulating (S) and recording (R) electrodes (S1 and S2 for callosal and local intracortical stimulation, respectively) on the slice and the various anatomical structures that can be easily recognized: CC stands for the corpus callosum and CA1, CA3 are regions of the hippocampus. Roman numerals indicate cortical laminae.

recording chamber such that the "liquid filament," generated at the interface between solutions flowing through the barrels of the θ tube, was roughly orthogonal to the patch electrode (Fig. 7*A1*). Because the liquid filament was visible only under conditions when solutions flowing out through the chambers of the θ tube were of different optical densities [normal rat Ringer (NRR) and 10% NRR], the final location of the patch pipette within the streams was determined prior to actual experimentation. Responses with the shortest rise times without overshoot (<0.1 ms, Fig. 7*A2*) were obtained when the patch pipette was placed ~100–120 μm from the edge of the θ tube and at a perpendicular distance of ~50–60 μm from the liquid filament. It was essential that the flow rate through the chambers of the θ tube be constant (80–120 μl/min), and this was achieved either through a syringe pump (Sage Instruments, White Plains, NY) or via gravity. Rapid exchange of as many as three different solutions in each of the chambers was made possible by running three independently primed lines from the solution reservoirs to four-way Teflon manifolds whose outputs were fed directly to the two barrels of the θ tube. All solutions used in the rapid application experiments were HEPES buffered. The control solution (NRR, in mM: 135 NaCl, 5.4 KCl, 1.8 $CaCl_2$, 1 $MgCl_2$, and 5 HEPES; pH adjusted to 7.3 with NaOH) usually flowed through one barrel and the test solutions through the other. The duration of the solution change was controlled by a home-made computer-interfaced piezo-controller (CCP96). For fast application of the agonist, freshly prepared L-glutamate (30 μM) was added to the NRR. For Ca^{2+} permeability experiments, the test solution was com-

prised of (in mM) 100 $CaCl_2$, 1 $MgCl_2$, and 5 HEPES; pH adjusted to 7.3 with $Ca(OH)_2$. To block NMDAR-mediated currents, 40 μM D-APV was added to all solutions. NBQX (10 μM) was used with NRR to antagonize AMPAR-mediated responses (Fig. 7*B*). Membrane currents were recorded with an Axopatch 1D, filtered at 2 kHz, digitized, and stored on-line. Reversal potentials were estimated from current-voltage (*I-V*) relations by linear interpolation.

RESULTS

Callosal stimulation and connectivity

Pyramidal neurons in layer V of the agranular frontal cortex were whole cell voltage clamped at −70 mV (Fig. 1*A1*). Stimulation of the corpus callosum, close to the midline, evoked an inward EPSC in >70% of the recorded pyramidal neurons, suggesting a relatively high intrahemispheric connectivity in this region. Responses in a given neuron could only be evoked from within a narrow region of the fiber track, and they were dependent on the location of the stimulating electrode (Fig. 1, *A1–A5*) or the intensity of stimulation. Optimal stimulating electrode placement was defined as the position on the callosal track from where a maximal all-or-none response could be evoked using the lowest stimulus intensity (100–500 μA; Fig. 1*A2*). EPSCs could also be successfully evoked from portions of the callosal track extending into the contralateral hemisphere indicating that the integrity of the pathway was preserved across the midline (Fig. 1*A5*). However, the chances of finding a callosally connected pyramidal neuron were greatest close to midline in the agranular frontal cortices (Fr1 and 2) (Paxinos and Watson 1986), although we have recorded callosal responses from cells in more lateral regions such as the sensorimotor cortex (Fig. 1*A1*). These differences in connectivity may have arisen either due to the severing of axons

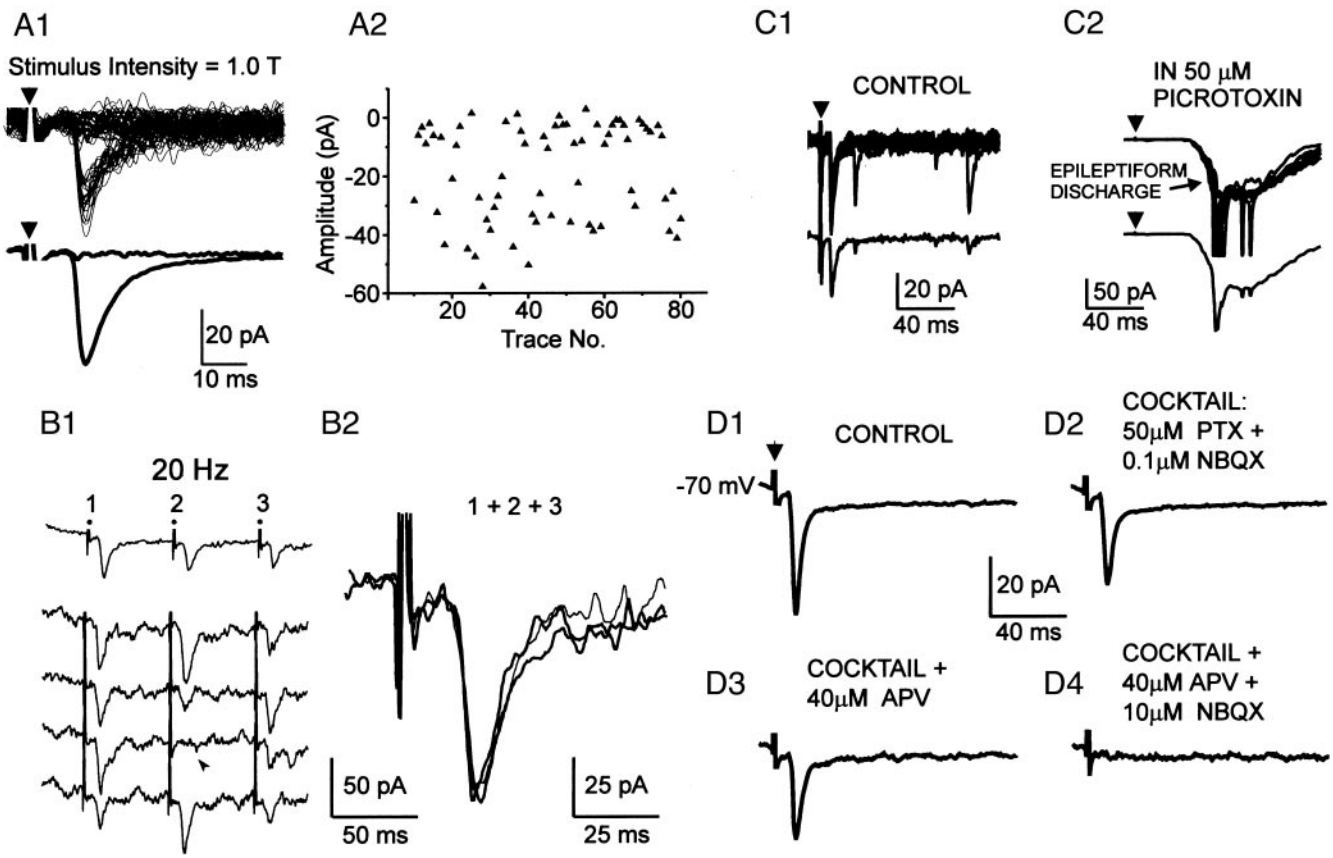

FIG. 2. Single fiber responses and the pharmacological scheme for isolating purely excitatory postsynaptic currents (EPSCs). *A1* and *A2*: example of superimposed (*top*, *A1*) and averaged (*bottom*, *A1*) responses evoked at threshold (*T*). Note the all-or-none nature of the response as reflected in the occurrence of intermingled successes and failures. Note also the fixed latency of the successes from respective stimuli (arrows). A plot of the variability in response amplitude as a function of stimulus number is shown in *A2*. *B*: preservation of EPSC characteristics during high-frequency stimulation (3 impulses, 20 Hz.). *B1*: average of the 10 consecutive responses (0.2 Hz.), 4 of which are shown below. The arrowhead points to a failure, and the numbered symbols represent stimuli. Averaged responses from the 1st, 2nd, and 3rd stimuli with normalized peak amplitudes superimposed in *B2* to show their fixed latency from stimulus onset and similarities in their kinetic properties. *C*: multiple superimposed (*top*) and averaged (*bottom*) PSCs evoked at 1.2*T* (−70 mV) in control artificial cerebrospinal fluid (ACSF; *C1*) and subsequently after the addition of 50 μM picrotoxin (PTX) to the bathing medium (*C2*). Note the resulting epileptiform discharge. *D*: pharmacological scheme used to isolate pure excitatory EPSCs. PTX was used to block $GABA_A$-mediated inhibition and low 2,3-dihydro-6-nitro-7-sulfamoyl-benzo(F)quinoxaline (NBQX; 0.1 μM) to reduce excitation and prevent hyperexcitability (*D2*). Note the ~20% reduction in peak amplitude of the response under these conditions. EPSCs were evoked under minimal stimulation conditions and deemed monosynaptic based on their fixed latency and ability to follow high-frequency stimulation without changes in their kinetic properties (not shown). Note that D(−)-2-amino-5-phosphonopentanoic acid (D-APV) has no effect (−70 mV, *D3*), while increasing the concentration of NBQX to 10 μM blocked the response (*D4*), suggesting a purely α-amino-3-hydroxy-5-methyl-4-isoxazolepropionic acid receptor (AMPAR)–mediated response at this holding potential.

during slice preparation or the inhomogeneous distribution of the callosal connections in these areas of the neocortex (Ivy and Killackey 1981; Olavarria and Van Sluyters 1986).

Stimulus intensity was increased until a threshold (*T*) for evoking the EPSC could be established and kept just above the threshold level (~1.2*T*), where no further change in response amplitude could be detected, for the duration of the experiment. In a majority of cases, the threshold was characterized by the occurrence of frequent failures, as shown in Fig. 2, *A1* and *A2*. Under these conditions callosal stimulation most likely activates a single axon collateral (*minimal stimulation*) since increasing stimulus intensity presumably recruits more fibers contributing to an increase in response amplitude and could lead to activation of polysynaptic responses as reflected by changes in the EPSC kinetics. In a few cases, a biphasic response, comprised of two overriding PSCs, was observed such that both components had fixed latencies from stimulus onset and shared the same threshold for activation (data not shown). These most likely represented cases in which pairs of axon collaterals making synaptic contacts with the recorded neurons were simultaneously activated because neither component dropped out when stimulus frequency was increased. EPSCs evoked by minimal stimulation of the callosum had an averaged peak amplitude of 56.5 ± 5.3 (SE) pA and a latency of 6.13 ± 0.2 ms from stimulus onset ($n = 31$). These were most likely monosynaptic by virtue of their ability to follow stimulus trains of 1–20 Hz without changes in either their latency or kinetic properties (Fig. 2, *B1* and *B2*) (Dobrunz and Stevens 1997; Lambert and Wilson 1993).

To study excitatory responses in isolation and reduce contribution from polysynaptic connections, picrotoxin (PTX, 50 μM) was included in the bathing medium to block all $GABA_A$ receptor–mediated responses and Cs^+ in the internal solution to block $GABA_B$ responses. However, the complete absence of inhibition usually resulted in tissue hyperexcitabilty (Fig. 2*C2*), which could be controlled and prevented by adding a low concentration (0.1 μM) of the AMPA/kainate receptor antagonist NBQX to the perfusate. In the presence of the PTX, low-NBQX "cocktail," the peak response amplitude was reduced by 20%, and EPSCs evoked under these conditions (−70 mV) could be completely abolished by increasing the concentration of NBQX to 10 μM, indicating that they were mediated by AMPA/kainate receptors (Fig. 2*D*). Since the expression of kainate receptors in the neocortex is substantially reduced after *postnatal day 7* (*P7*) and kainate receptor–mediated EPSCs have larger decay time constants (Kidd and Isaac 1999) compared with responses isolated in this study, the latter were likely mediated predominantly by the AMPA class of ionotropic glutamate receptors.

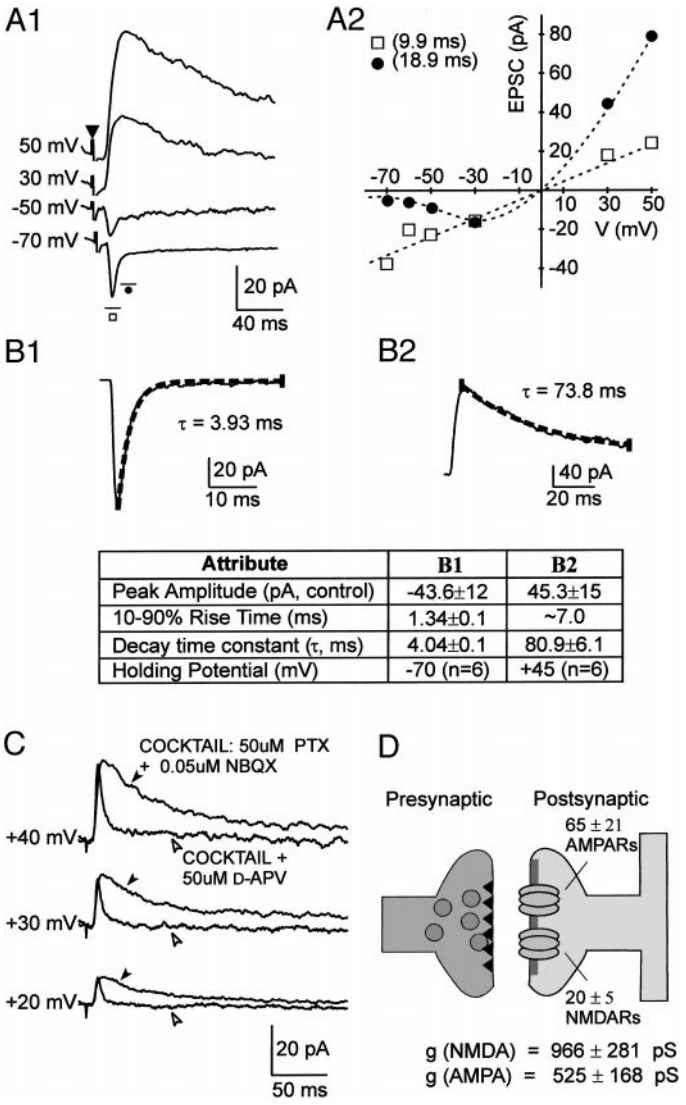

Attribute	B1	B2
Peak Amplitude (pA, control)	-43.6±12	45.3±15
10-90% Rise Time (ms)	1.34±0.1	~7.0
Decay time constant (τ, ms)	4.04±0.1	80.9±6.1
Holding Potential (mV)	-70 (n=6)	+45 (n=6)

FIG. 3. Physiological properties of callosally evoked EPSCs. *A*: typical responses isolated in cocktail at the indicated holding potentials (*A1*). The *N*-methyl-D-aspartate receptor (NMDAR)–mediated component is revealed on depolarization as confirmed by the current-voltage relationship (*A2*). Traces are averages of 10 or more responses, and series resistance was constant at ~5 MΩ throughout the experiment. All recordings are obtained at 32°C. *B*: kinetic properties of callosal EPSCs. Traces are fit with a 1st-order single exponential function, and summary information in the boxes represents average values from recordings obtained between *P12* and *P15* ($n = 6$). *C*: the late, slowly decaying NMDAR-mediated component of the callosal EPSC evoked during minimal stimulation can be distinguished from AMPA at the depolarized holding potentials by its blockade with 50 μM D-APV. *D*: estimates of the number of AMPA and NMDA receptors per synapse (assuming minimal stimulation activates a single synapse) obtained from measurements of the respective conductances (derived from the current-voltage relationships) and single-channel conductance information (see text for references).

Voltage dependence of callosally evoked EPSCs

To determine the *I-V* relationship of the pharmacologically isolated callosal EPSCs, we measured the magnitude of both early and late components at various holding potentials in the range −80 to +50 mV in the presence of the cocktail (Fig. 3*A1*). The *I-V* plot of the early component of the response, corresponding to the peak inward current at −70 mV (a latency of 9.9 ms from stimulus onset in the experiment in Fig. 3*A2*, □), reversed near 0 mV and was linear in mature tissue (>*P15*) but showed inward rectification in younger animals (discussed further in section on developmental changes). The short duration of the responses observed at hyperpolarized holding potential (−70 mV) together with their 10–90% rise time and decay time constant (τ) of 1.34 ± 0.1 ms and 4.04 ± 0.1 ms ($n = 6$), respectively, were consistent with an AMPAR-mediated current. In contrast, the late component of the response, recorded at a latency of 18.9 ms (Fig. 3*A2*, ●), in the example illustrated, decayed more slowly ($\tau = 80.9 \pm 6.1$ ms, $n = 6$) and was activated only at depolarized potentials (greater than

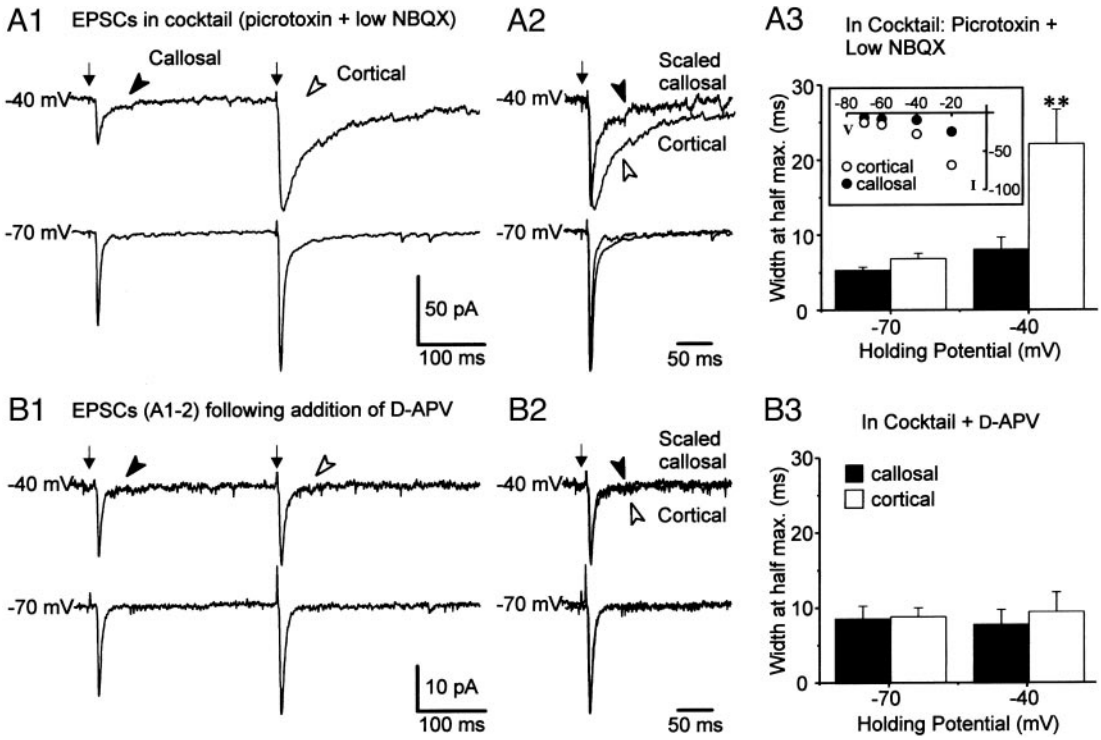

FIG. 4. Stimulation of callosal and local inputs reveals input and/or age-specific differences in NMDAR-mediated responses. *A1* and *A2*: averaged single-fiber EPSCs (isolated in cocktail from a *P14* neuron) evoked at 2 different holding potentials by alternately stimulating the callosum (filled arrowheads) and locally (open arrowheads). Note how the NMDAR-mediated component of the local cortical response is activated at a more hyperpolarized holding potential compared with the one activated by callosal stimulation (*A1*). Responses normalized to the peak amplitude are shown in *A2*. Note that differences in the decay kinetics of the EPSCs are manifest at −40 mV but not at −70 mV. *A3*: response duration vs. holding potential for callosal and cortical responses averaged from 4 experiments under the above conditions. *B*: EPSCs recorded from the same neuron (*A1* and *A2*) following the addition of 50 μM D-APV to the bathing medium. All traces are averages of >20 responses evoked at 0.2 Hz, and arrows point to stimuli. *B3*: effects of APV on EPSC duration for callosal and cortical responses in the experiments depicted in *A3*. The *inset* in *A3* is an *I-V* relationship of the late NMDAR-mediated components of the callosal (●) and intracortically (○) evoked EPSCs (*A1* and *A2*), showing difference in the holding potentials (*V*, mV) at which they are activated and their amplitudes (*I*, pA). ** $P < 0.05$.

−40 mV), characteristic of an NMDAR-mediated current and its blockade by Mg^{2+}. A comparison between the properties of representative inward (−70 mV) and outward responses (+45 mV) is shown in Fig. 3, *B1* and *B2*. AMPA and NMDAR-mediated components contributing to the EPSC could be further disassociated by using receptor-specific antagonists. Figure 3*C* shows the effect of the NMDAR antagonist D-APV (50 μM) on the amplitude and kinetics of EPSCs evoked at the various depolarized holding potentials indicated. Note that in the presence of D-APV, a late, slowly decaying component of the response originally present in the cocktail solution (filled arrowheads) was transformed into a faster and briefer response (open arrowheads) typical of AMPA receptors. These data suggest that minimal stimulation of the callosum evokes mixed EPSCs with both AMPA and NMDAR-mediated components.

Receptor composition of a callosal synapse

Characterization of the *I-V* relationship underlying the callosal response and its components enabled the determination of not only the receptor composition of these synapses but an estimation of the number of receptors contributing to the putative monosynaptic response as well. Single-channel conductance estimates for the AMPAR in the literature have ranged from ~8 pS (Benke et al. 1998) to ~20 pS (Traynelis et al. 1993). In the present study, conductance measurements for the AMPAR-mediated component of the EPSC, based on the slope of the linear fit of the *I-V* relationship, averaged 525 ± 188 pS ($n = 6$). This corresponds to between 26 and 65 AMPA receptors per synaptic contact (Fig. 3*D*). Similarly, the averaged conductance associated with the NMDARs, based on the late component of the EPSC at a holding potential of +40 mV, was estimated at 966 ± 281 pS ($n = 6$) and corresponds to ~20 NMDA receptors per synaptic contact, assuming a single NMDAR channel conductance of ~50 pS (Cull-Candy et al. 1988). These estimates, however, do not take into account the stochastic nature of channel opening and are likely to represent the lower limits of their ranges in vivo given the pharmacologically reduced nature of the preparation.

Comparison between the kinetic properties of callosal and noncallosal AMPA responses

To determine whether the functional properties of the callosal projections onto layer V pyramids were unique to this pathway, we compared the kinetics of the callosally evoked EPSCs with those evoked by local intracortical stimulation. Intracortical stimulation activates a variety of excitatory afferents, including short-range axons, making synaptic contacts with the pyramidal neuron that are at least partially different from those activated during callosal stimulation. A second stimulating electrode was positioned in the vicinity of the

recorded neuron, either on- or off-column, and a stimulation paradigm similar to the one described for callosal stimulation was used to evoke intracortical EPSCs in the pyramidal neuron (Fig. 1*B*). Intracortical EPSCs had shorter latencies from stimulus onset when compared with those evoked by callosal stimulation (3.1 ± 0.2 ms vs. 6.1 ± 0.2 ms, $n = 14$, $P < 0.001$). However, in the presence of D-APV, the 10–90% rise times for intracortically evoked EPSCs (2.3 ± 0.3 ms) and those evoked by callosal stimulation (2.3 ± 0.2 ms) were similar at both −70 mV and at depolarized holding potentials between +40 and +60 mV (2.34 ± 0.3 ms vs. 2.7 ± 3.3 ms; $P > 0.5$, $n = 14$). Likewise, the decay time constants for intracortical and callosal EPSCs were also similar (7.1 ± 0.5 ms vs. 6.8 ± 0.5 ms) at −70 mV, although the former had larger τs at positive holding potentials compared with the latter (9.8 ± 0.9 ms vs. 7.2 ± 0.5 ms, $P < 0.05$). These data suggest that the postsynaptic properties of AMPAR-mediated EPSCs are common to all synapses of layer V pyramids.

Input-specific differences in the NMDA receptor–mediated component of the EPSC

To determine whether the lack of input specificity observed with AMPAR-mediated responses also extended to NMDARs, we compared callosal and intracortical EPSCs evoked in the same pyramidal neurons at two different holding potentials using the alternate stimulation protocol described above. Figure 4 shows trace averages of 10 or more consecutive responses at −40 and −70 mV in the presence of the PTX and low-NBQX cocktail. At −70 mV, callosal and intracortical EPSCs were indistinguishable in terms of their kinetic properties, except for differences in their latencies from stimulus onset. Depolarization to −40 mV reduced the amplitude of both responses, presumably as a result of reduction in the driving force, but the intracortically evoked EPSCs decayed at a significantly slower decay rate than the EPSCs evoked by callosal stimulation. Figure 4*A2* shows the two responses normalized and superimposed to reveal differences in their kinetic properties. Note that, while both EPSCs had similar rise times at the two holding potentials, their decay time constants at −40 mV are strikingly different. The average widths at half-maximum amplitude for the callosal response at −70 and −40 mV were 5.3 ± 0.4 and 8.1 ± 1.6 ms, respectively, in contrast with 6.8 ± 0.7 and 22.1 ± 4.6 ms for intracortical stimulation ($P < 0.05$, $n = 4$; Fig. 4*A3*). The addition of 50 μM D-APV to the perfusate blocked the slowly decaying component of the intracortically evoked response at −40 mV, while leaving the rapidly decaying response unaffected (Fig. 4*B1*). The scaled traces in the presence of D-APV were now similar for both stimulus paradigms (Fig. 4*B2*), suggesting that the differential response was mediated by NMDARs. The widths at half-maximum amplitude for the callosal and intracortical responses at −70 and −40 mV were comparable in the presence of D-APV, averaging 8.6 ± 1.7 and 7.9 ± 1.9 ms for the callosal and 8.9 ± 1.2 and 9.6 ± 2.6 ms for intracortical stimulation, respectively ($n = 4$; Fig. 4*B3*). The pathway-specific NMDAR responses at callosal versus intracortical synapses could be due to differences in either the voltage dependence of the underlying NMDARs or in the relative numbers of AMPARs versus NMDARs. Preliminary evidence suggests that the voltage dependence of intracortical responses is shifted in the hyperpolarized direction compared with callosal synapses (Fig. 4*A3*, *inset*), but future studies will be required to fully characterize the differences in the properties of NMDARs at the two synapses as well as the relative contributions of AMPARs versus NMDARs.

Rectification properties of AMPAR-mediated I-Vs change during development

The pure AMPAR-mediated responses in cortical pyramidal neurons from animals older than *P15* were characterized by linear *I-V* relationships that reversed close to the expected reversal potential of 0 mV as shown in Fig. 5*A*. The average rise times and decay time constants for EPSCs at the depolarized holding potentials were similar to those at hyperpolarized levels, and all responses could be completely blocked by increasing the concentration of NBQX to 10 μM in the perfusate. By contrast, *I-V* relationships in neurons from younger animals (<*P16*) were inwardly rectifying (Fig. 5*B*). The rectification index (RI), defined as the ratio of AMPA conductances measured at +40 and −70 mV, varied widely for neurons from animals between *P13* and *P15* (range, 0.3–1.6), but on average (0.7 ± 0.11, $n = 12$) was smaller than the RI for the older *P16–21* age group (1.2 ± 0.13, $n = 11$, range = 0.6–1.8; $P < 0.01$; Fig. 5*C*).

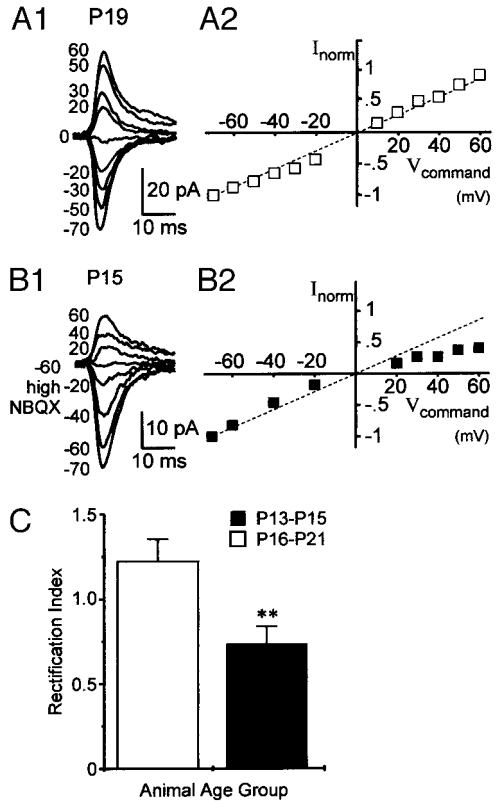

FIG. 5. Age-related variations in the rectification properties of AMPAR-mediated *I-Vs*. *A*: averaged AMPAR-mediated currents (isolated in 80 μM D-APV) at the indicated holding potentials and the corresponding peak current-voltage relationship for a *P19* neuron. *B*: data from a *P15* neuron showing an inwardly rectifying *I-V* relation. EPSCs in both *A2* and *B2* were normalized to their amplitudes at −70 mV, and voltages were corrected for a junctional potential of ~10 mV. The hatched line represents a unitary rectification index. *C*: bar plot of the averaged rectification indexes in the age groups indicated. ** $P < 0.001$.

Spontaneously occurring EPSCs

Given that properties of AMPA and NMDAR-mediated EPSCs evoked in layer V pyramids may be different in terms of their input specificity, we attempted to explore these relationships further by examining the properties spontaneously occurring EPSCs (sEPSCs) recorded in these neurons. As intracortically evoked EPSCs belong to the same heterogeneous population of responses as the spontaneous events, we expected their functional properties to be similar. To test this hypothesis, sEPSCs recorded from neurons under identical conditions as those during intracortical or callosal stimulation were analyzed and compared at the holding potentials of ±40 mV (Fig. 6, *A1* and *A2*). Figure 6*A1* shows examples of records obtained from a *P19* neuron under the indicated pharmacological conditions juxtaposed with their respective averages. The bulk of the sEPSC population under control conditions (−70 mV, in ACSF) was almost entirely mediated by AMPARs as the addition of NBQX to the bath blocked all events (data not shown). AMPAR-mediated responses were isolated in cocktail, and D-APV and could be easily identified as inward or outward events depending on the holding potential (±40 mV, arrowheads).

We observed that the frequency of spontaneous events was generally higher in older as opposed to the younger animals, and sEPSCs in animals *P15* or younger could most often be successfully detected only at −40 mV but not at the depolarized holding potential +40 mV (Fig. 6*A2*). These differences may be attributable to the same factors responsible for the age-dependent rectification of the evoked AMPAR-mediated EPSCs observed in the younger animals. The rise times and τs for sEPSCs recorded at −40 mV in these animals were similar to those observed in the older age group (rise time: 1.55 ± 0.2 ms vs. 1.56 ± 0.3 ms, $P = 0.97$; τ: 4.93 ± 0.7 ms vs. 4.24 ± 0.6 ms, $P = 0.44$). For animals older than *P15*, the amplitudes and rise times of sEPSCs recorded at ±40 mV were also comparable (35.4 ± 9.3 pA vs. 31.85 ± 12.7 pA; 1.57 ± 0.2 ms vs. 1.56 ± 0.3 ms; $n = 8$ and 7; $P = 0.83$ and 0.97, respectively), except for τ, which was larger at +40 mV as opposed to −40 mV (8.44 ± 1.0 ms vs. 4.24 ± 0.6 ms; $P < 0.005$). Spontaneous events (±40 mV) could be blocked by NBQX (10 μM), indicating that they were mediated by AMPARs.

The averaged peak amplitude of sEPSCs recorded at ±40 mV in the presence of D-APV (Fig. 6*B*) was similar to the callosally evoked EPSCs at the same holding potentials (HP_{-40}: −35.4 ± 9.2 pA vs. −29.9 ± 7.3 pA; HP_{+40}: 31.9 ± 12.7 pA vs. 25.9 ± 4.9 pA, $n = 9$; $P > 0.5$). However, while the rise times for the evoked responses were significantly larger than those for the sEPSCs (HP_{-40}: 2.2 ± 0.2 ms vs. 1.6 ± 0.3 ms; HP_{+40}: 2.9 ± 0.5 ms vs. 1.6 ± 0.2 ms, $n = 8$; $P = 0.02$ and 0.04, respectively) at both holding potentials, the decay time constants were similar (HP_{-40}: 5.9 ± 0.7 ms vs. 4.2 ± 0.6 ms; HP_{+40}: 7.4 ± 0.7 ms vs. 8.4 ± 0.9 ms, $n = 8$; $P > 0.1$). Thus based on decay kinetics, callosally evoked AMPAR-

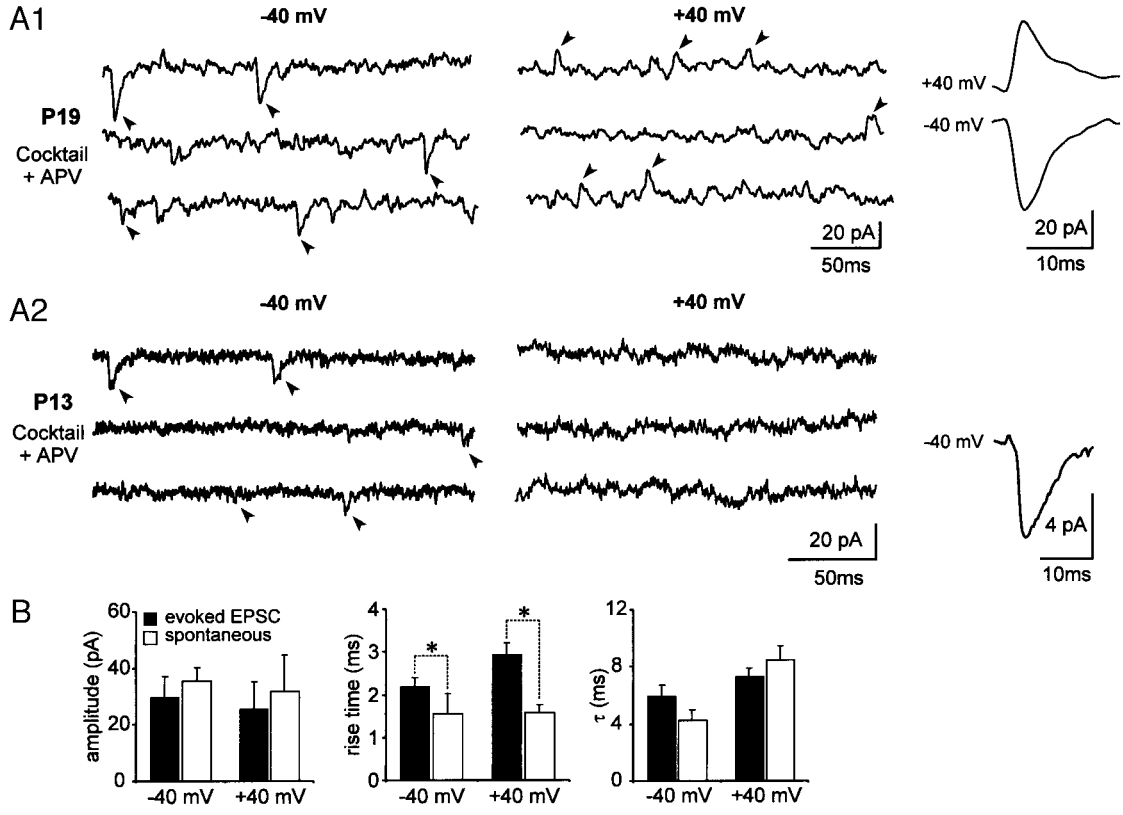

FIG. 6. Properties of spontaneously occurring EPSCs. *A*: prototypic responses recorded at ±40 mV in a *P19* neuron (*A1*) and a *P13* neuron (*A2*) under the indicated pharmacological conditions. Averages of the events detected (arrowheads) are presented juxtaposed with the sweeps. Elevating NBQX in the bath to 10 μM abolished all responses in *A1* and *A2*, indicating that they were mediated by AMPA receptors (not shown). Note that spontaneous events could be detected at both ±40 mV only in the older animal but not in the younger (*P13* and *A2*). *B*: bar plots comparing amplitudes, rise times, and decay time constants of spontaneous and evoked EPSCs at the 2 potentials (±40 mV).

mediated EPSCs were comparable to sEPSCs recorded in the same neurons under the identical conditions. The observed differences between the rise times for the evoked and spontaneous data might be explained in terms of differences in the location of the activated synapses on the neuron and the differential electrotonic filtering of callosal responses.

Somatic versus synaptic receptors

The observation that both spontaneous and evoked AMPAR-mediated EPSCs in the younger (<*P16*) animals display similar age-dependent differences in rectification compared with the older animals suggests that physiological properties of the underlying receptors at these ages might be different. We recently demonstrated that synaptic AMPARs in the younger animals lack the GluR2 subunit thereby affecting linearity of their *I-V* relationships and making them permeable to divalent cations, most notably Ca^{2+} (Kumar et al. 2001). However, a variety of experimental data, including that derived from outside-out patches, has suggested that Ca^{2+}-permeable AMPARs lacking GluR2 are expressed predominantly by GABA-ergic interneurons but not principal cells (Geiger et al. 1995; Jonas and Burnashev 1995; Jonas et al. 1994; McBain and Dingledine 1993; Washburn et al. 1997; Yin et al. 1999). The results with synaptic AMPA responses reported here suggest the alternate possibility that synaptic AMPARs may be functionally distinct from those located on the soma. To test this hypothesis, we used outside-out patches excised from the somas of pyramidal cells in young animals to directly assay Ca^{2+} permeability through somatic receptors by measuring the shift in reversal potential of agonist-activated currents produced by different extracellular Ca^{2+} concentrations (see METHODS). The reversible blockade of the glutamate-evoked control responses by NBQX as shown in Fig. 7*B* confirms the activation of AMPARs. Under conditions of normal extracellular Ca^{2+} (1.8 mM) the *I-V* relationship of the glutamate-evoked responses obtained by varying the holding potential reversed close to 0 mV as expected (Fig. 7*C1*). In contrast, when the extracellular concentration of Ca^{2+} in the bath was raised to 100 mM, the inward currents diminished substantially, and the reversal potential shifted to more hyperpolarized potentials (Fig. 7*C2*), indicating impermeability of Ca^{2+} through these receptors (Fig. 7*D*). We observed this shift in reversal potential consistently in all of five experiments with an average shift of -61.9 ± 1.9 mV, which corresponds to a calculated Ca^{2+} to Na^+/Cs^+ permeability ratio of 0.04 estimated using the Goldman-Katz equation (Jonas and Sakmann 1992; Lewis 1979; Mayer and Westbrook 1987). This contrasts with the higher permeability ratio estimated from synaptic responses (>2, Kumar et al. 2001) but is consistent with anatomical observations (Carder 1997; Lerma et al. 1994; Yin et al. 1999) and suggests phenotypic differences between the subunit composition of AMPARs located at the soma and the synapse.

Paired stimuli

Paired stimuli applied to the callosum at a frequency of 0.2 kHz were used to evoke dual responses in the layer V pyra-

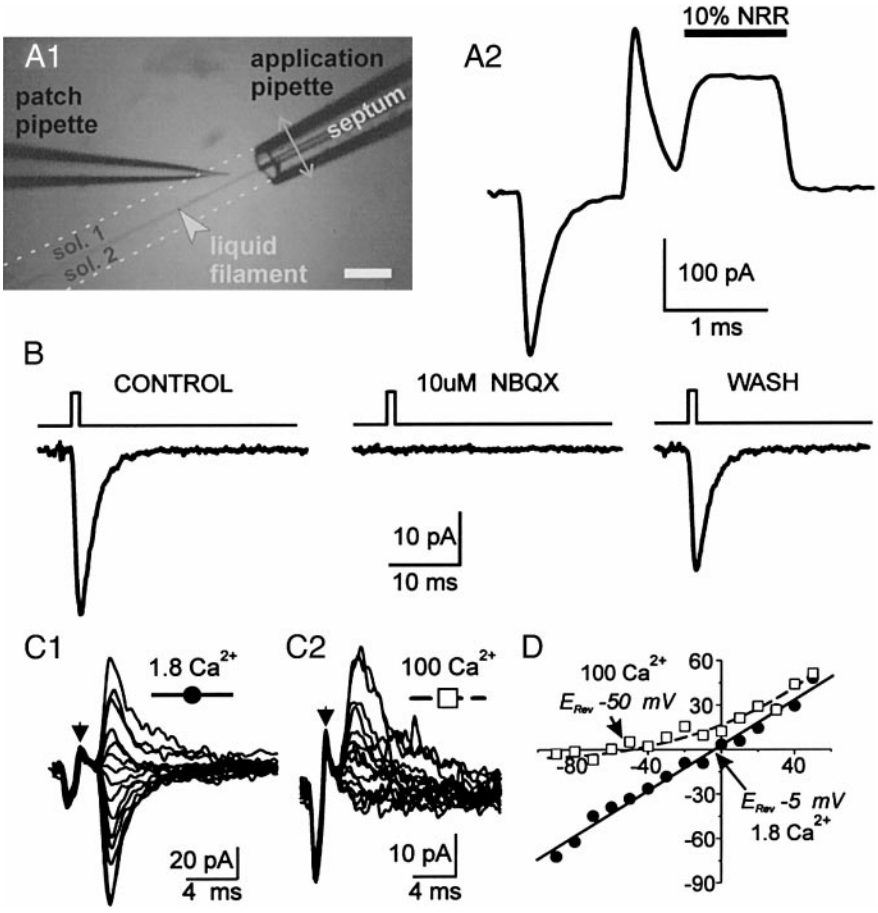

FIG. 7. Outside-out patches from young animals (<*P16*) contain AMPARs that are impermeable to Ca^{2+}. *A1*: schematic of the experimental arrangement showing the position of the patch pipette with respect to application pipette (theta-tube) mounted on a piezo device and the liquid filament generated due to the flow of normal rat Ringer (NRR) and 10% NRR through the barrels of the theta tube, respectively. *A2*: change in junction potential recorded by a rapid step movement of the theta-tube such that the liquid filament crossed the tip patch pipette for the duration desired, typically 1 ms. Note that the early response represents a biphasic artifact, resulting from the charging of the piezo device, followed by the pulse response with a short rise time and ~1 ms in duration resulting from change of solutions (NRR → 10% NRR, bar). *B*: typical responses recorded from patches during brief applications (1 ms) of glutamate (30 μM) under the indicated conditions. NBQX reversibly antagonizes the responses. *C1* and *C2*: averages of agonist-evoked currents generated at various holding potentials between −90 and +50 mV with 1.8 mM Ca^{2+} in the bath (*C1*), and following elevation to 100 mM (*C2*). Responses in *C1* and *C2* are from different patches taken from the same neuron. Note the reduction in inward currents and the leftward shift in the reversal potential of the corresponding *I-V* relationship (arrows in *D*). Physiological responses resulting from a 1-ms exposure of patches to glutamate in *C1* and *C2* immediately follow termination of the piezo-charging artifact (arrows).

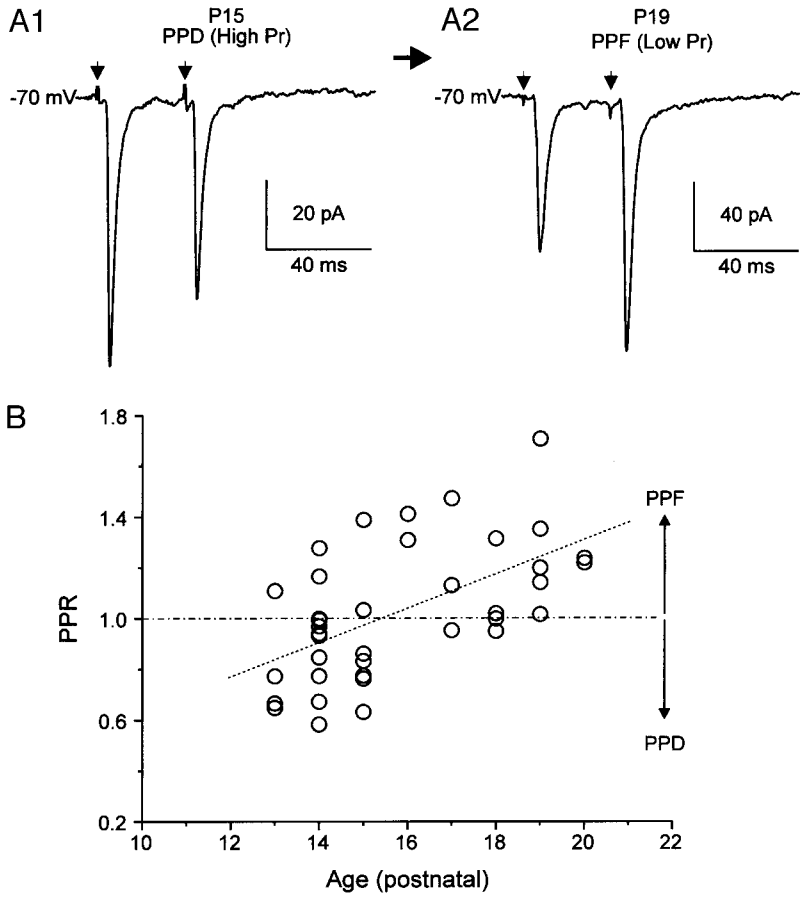

FIG. 8. Conversion of paired-pulse depression to facilitation suggests alterations in presynaptic release properties and/or properties of postsynaptic receptors at a maturing synapse. *A1* and *A2*: paired stimuli separated by 50 ms used to estimate paired-pulse depression (PPD) and/or facilitation (PPF) in animals in the range of *P13–P20*. PPD/F are estimated using the relationship [(response 2 − response 1)/response 1]. Traces are averages of ~20 responses, and the scatter plot in *B* indicates the % change in the 2nd response compared with 1st as a function of postnatal age. One-way repeated measures ANOVA indicates statistically significant differences in the paired-pulse ratios with development ($P < 0.05$).

midal neurons with the aim of assaying presynaptic release properties at the callosal synapse. We found that the response characteristics to this stimulation paradigm were again dependent on animal age such that animals *P15* or younger were dominated by paired-pulse depression (PPD), while animals older than *P15* generally showed paired-pulse facilitation (PPF; Fig. 8). The paired-pulse ratio (PPR), defined as the ratio of the second response divided by the first, averaged 0.89 ± 0.04 ($n = 22$) for animals between *P13* and *P15* and was significantly smaller than the averaged PPR for the older *P16* through *P20* animals 1.22 ± 0.05 ($n = 16$, $P < 0.0001$, *t*-test). Figure 8, *A1* and *A2*, shows representative trace averages of 20 or more consecutive responses from animals in the age groups *P15* and *P19*. The scatter diagram in Fig. 8*B* shows the PPR as a function of animal age. Thus while the second response in a *P13* animal was depressed by 20.4 ± 10.8% ($n = 4$) when compared with the first, the equivalent response in a *P19* animal was facilitated by 28.4 ± 11.9% ($n = 5$). As shown on the plot in Fig. 8*B*, the transition in the response characteristics of layer V pyramidal neurons to paired stimuli from PPD to PPF can be estimated from the point of intersection between the linear best fit of the combined data (dotted, $R = 0.56$, $n = 38$) and the 0% change reference (stippled line). Changes in PPR are usually taken as indicators of alterations in presynaptic release properties (Dobrunz and Stevens 1997; Goda and Stevens 1998) with PPD and PPF designating synapses with high and low probability of transmitter release, respectively (reviewed in Thomson 2000). Despite the use of a fixed stimulus frequency in the above experiments and the possibility that changes in paired-pulse ratio may depend on the choice of the interstimulus interval (Thomson and West 1993), the transition from mainly PPD in the young animals to PPF in the older age group suggests that the presynaptic release properties at callosal synapse may vary during development. However, our data do not preclude the possibility of an entirely postsynaptically mediated change, for example through an alteration of the desensitization properties (Pelletier and Hablitz 1994; Rozov and Burnashev 1999) of the underlying receptors, or a combination of the two possibilities (Thomson et al. 1993).

DISCUSSION

Reductionist models of cortical function are necessitated in part by the complexity of underlying neural circuitry. In this report we have attempted to investigate whether the e-e connections of the corpus callosum can serve as a model system for the study of intracortical (cortico-cortical) excitability. Despite the fact that the corpus callosum has been a very well studied structure anatomically (Innocenti 1986; Pandya and Seltzer 1986), the functional and physiologic properties of callosal projections have remained poorly characterized. Previous electrophysiological studies have been necessarily incomplete due in part to the nonavailability of modern techniques in the past as well as due to the difficulty of preserving intra-hemispheric callosal connectivity in an in vitro slice preparation owing to the curvature of the callosum. Furthermore, the study of pure excitatory responses in isolation has remained a challenge due to the complications of hyperexcit-

ability that results from the complete blockade of inhibition in the tissue (Avoli et al. 1997; Sutor and Luhmann 1998). Our goal was thus to overcome these difficulties to allow an objective assessment and characterization of the basic biophysical properties of callosally mediated synaptic currents and to compare these with other noncallosal excitatory inputs to validate the use of the callosal model for the study of excitatory cortico-cortical connections in the neocortex.

In a previous study Kawaguchi (1992) reported that transcallosal potentials in layer V pyramidal neurons were mediated by an early excitatory postsynaptic potential (EPSP) followed by a dual component inhibitory postsynaptic potential (IPSP) that most likely involved the activation of GABA-ergic ($GABA_A$ and $GABA_B$) interneurons. GABA-mediated responses were pharmacologically blocked in the present study. Some neurons recorded in a previous study in the posterior cingulate cortex showed significant hyperpolarizing afterpotentials usually followed synaptically evoked spikes and required a much stronger stimulation of the callosum (Vogt and Gorman 1982). Similar observations by Thomson (1986) suggest that, at lower stimulus intensities, EPSPs can be evoked alone without the manifestation of an accompanying IPSP. Furthermore, while the earlier studies (Kawaguchi 1992; Thomson 1986) were successful in demonstrating that 6-cyano-7-nitroquinoxaline-2,3-dione (CNQX; a non-NMDAR antagonist) blocked all transcallosal potentials, indicating the direct involvement of AMPARs, evidence for NMDAR has been particularly lacking. The NMDAR antagonist D-APV did not produce consistent changes in any of the synaptic potentials, and it required prolonged incubations of the preparation in Mg^{2+}-free solution to reveal the late depolarizing component of the transcallosal response that is typical of NMDARs. Thus, based on electrophysiological criteria alone, it was not possible to determine whether NMDARs of layer V neurons were activated monosynaptically by callosal fibers or indirectly through other cortical neurons (Conti and Manzoni 1994). Interestingly, intracortical (IC), as well as thalamocortical (TC), pathways were found to utilize both NMDA and non-NMDA receptors in adult animals (Gil and Amitai 1996). One likely explanation put forward by Kawaguchi why even strong depolarization could not demonstrate an NMDAR component to callosally induced EPSPs was that the large IPSP caused simultaneously by strong callosal stimulation prevented sufficient depolarization at the EPSC-generating sites to reveal the voltage-dependent NMDAR-mediated EPSP. While this possibility cannot be ruled out in the present study, as inhibition in the tissue was blocked entirely, depolarization of the neuron almost invariably brought out a late slowly decaying component that was blocked by D-APV (e.g., Fig. 3*C*). Thus callosal responses clearly have an NMDA component in layer V pyramidal neurons.

The minimal stimulation paradigm used for evoking single-fiber–mediated responses most likely activates both ortho- and antidromic callosal fibers, each of which would in turn activate monsynaptic excitatory connections onto the postsynaptic layer V pyramidal neuron. Hence this model consists of activation of a well-defined, relatively homogeneous population of intracortical excitatory connections. The averaged peak amplitude of the callosally evoked monosynaptic EPSC was larger than expected (56.5 ± 5 pA, −70 mV) but comparable with unitary evoked EPSCs measured in pyramidal cells in other areas of the neocortex (38.9 ± 21.2 pA at −60 to −70 mV) (Burgard and Hablitz 1993). Furthermore, the peak amplitudes of callosally evoked EPSCs were similar to spontaneous EPSCs recorded at the same holding potentials (−40 mV). The above comparison suggests that the amplitude of the callosal response most likely represents a quantal response despite the possible effects of dendritic filtering on either the amplitudes of the EPSCs or their kinetics. For example, the relatively slow rise times for the AMPA-mediated responses in the present study are probably due to the remote electrotonic location of the synapses on distal dendritic spines (Geiger et al. 1997; Hestrin 1997; Zhou and Hablitz 1997). In rabbits, sectioning the corpus callosum at birth led to the loss of dendritic spines that were restricted to the oblique branches of the apical dendrites of pyramidal cells in the adult animals, suggesting a distinct anatomical locus for the bulk of the callosal input onto these neurons (Globus and Scheibel 1967). These synapses were localized to the deep layer III and IV approximately 200–250 μm from the cell soma with an estimated passive attenuation factor of ~20% (Hausser and Roth 1997). Furthermore, spontaneous EPSCs were routinely obtained with rise times of <1 ms, indicating that the clamp-response time was adequate to obtain such measurements. Slow rise times and decay time constants have also been reported for synapses in the hippocampus (Hestrin et al. 1990; Jonas and Sakmann 1992; Keller et al. 1991), and measurements of these parameters for the callosal EPSCs were comparable with those reported for CA1 cell-synapses (rise time: 1.1–4.2 ms; τ: 4–8 ms) in particular, given the considerable variability between cells in different areas of the hippocampus.

The input specificity of various connections onto the pyramidal neurons is determined in part by the differences in the functional properties of the underlying receptors at these synapses. The AMPA components of callosally evoked EPSCs were similar in their kinetic properties to EPSCs evoked following the activation of local excitatory inputs. These data taken together with the observation that the former also could not be distinguished from sEPSCs recorded in the same neurons suggests that synaptic AMPARs on layer V pyramidal neurons are functionally similar. However, the failure to detect AMPAR-mediated sEPSCs at depolarized holding potentials in the young (*<P16*) animals cannot be explained by the lower overall frequency of spontaneous events in this age group alone, and suggest other possibilities related to developmental changes in receptor function such as inward rectification of synaptic currents also observed in this study for the evoked responses. In comparison, differences between callosal and noncallosal synaptic inputs appear to be more clear-cut with respect to the NMDA component, although it is necessary to examine whether these differences are also manifest throughout the various stages of early development as NMDARs may be subject to age-dependent alterations of their kinetic properties (Hestrin 1992). Alternatively, differences in NMDAR activation for the two types of excitatory connections may result from unique receptor subunit compositions and impart to the neuron the ability to distinguish the long-range callosal projections from the shorter ranged inputs arising locally (Burkhalter and Charles 1990; Johnson et al. 1996). Voltage-dependent differences in various types of NMDARs have also been previously reported for the robust TC and recurrent excitatory connections in spiny stellate neurons of layer IV in

mouse barrel cortex (Feldmeyer et al. 1999; Fleidervish et al. 1998). Pathway-specific differences can manifest not only through synaptic receptors but also via the presynaptic element as is the case with TC synapses, which have more release sites and a higher mean release probability than IC synapses and are differentially sensitive to presynaptic neuromodulators (Gil et al. 1997, 1999).

Developmental alterations in postsynaptic receptors may also change the dynamic properties of the synapse in a way that is normally associated with presynaptic function. For example, changes in paired-pulse ratios (e.g., Fig. 8) may result from alterations in AMPAR subunit composition (Rozov and Burnashev 1999). Reyes and Sakmann (1999) found that in the young cortex, the degree of synaptic depression in connected layer V pyramidal neurons was determined by whether the presynaptic cell was in layer II/III or V and that maturation of the cortex switched the depression of unitary EPSPs to facilitation (between *P14* and *P28*), thereby eliminating the layer-specific differences. The developmental changes in paired-pulse ratio reported here indicate the existence of a developmental program that alters the pre- and/or postsynaptic properties of the synapse by either modifying the pattern of transmitter release and/or changing the response properties of the postsynaptic element through alterations in receptor function. Whether these changes, which ultimately lead to alterations in synaptic efficacy, are associated solely with synapse maturation or can also be modulated by afferent activity remains to be determined. Finally, the age-specific changes observed in the present study add another degree of complexity to the analysis of intracortical responses and urge the need for caution in the interpretation of data from animals at different stages of development. Further, it is important to note that properties of somatic receptors may be distinct from those at the synapse. Thus data from outside-out patches in this study and previous analysis at the synaptic level (Kumar et al. 2001) demonstrate that somatic AMPARs, which are predominantly extrasynaptic on pyramidal neurons, differ physiologically from receptors at the synapse. It remains to be fully determined how this rich diversity of excitatory synaptic connections is exploited by individual pyramidal neurons during normal neuronal development and signal processing.

This study was supported by National Institute of Neurological Disorders and Stroke Grant NS-12151 and by an Epilepsy Foundation/American Epilepsy Society research training fellowship to S. S. Kumar.

REFERENCES

AKERS RM AND KILLACKEY HP. Organization of corticocortical connections in the parietal cortex of the rat. *J Comp Neurol* 181: 513–538, 1978.

ARAM JA AND LODGE D. Validation of a neocortical slice preparation for the study of epileptoform activity. *J Neurosci Methods* 23: 211–224, 1988.

AVOLI M, HWA G, LOUVEL J, KURCEWICZ I, PUMAIN R, AND LACAILLE JC. Functional and pharmacological properties of GABA-mediated inhibition in the human neocortex. *Can J Physiol Pharmacol* 75: 526–534, 1997.

BENKE TA, LUTHI A, ISAAC TR, AND COLLINGRIDGE GL. Modulation of AMPA receptor unitary conductance by synaptic activity. *Nature* 393: 793–797, 1998.

BRAITENBERG V AND SCHÜZ A. *Anatomy of the Cortex.* Berlin: Springer-Verlag, 1991.

BURGARD EC AND HABLITZ JJ. NMDA receptor–mediated components of miniature excitatory synaptic currents in developing rat neocortex. *J Neurophysiol* 70: 1841–1852, 1993.

BURKHALTER A AND CHARLES V. Organization of local axon collaterals of efferent projection neurons in rat visual cortex. *J Comp Neurol* 302: 920–934, 1990.

CARDER RK. Immunocytochemical characterization of AMPA-selective glutamate receptor subunits: laminar and compartmental distribution in macaque striate cortex. *J Neurosci* 17: 3352–3363, 1997.

COLQUHOUN D, JONAS P, AND SAKMANN B. Action of brief pulses of glutamate on AMPA/kainate receptors in patches from different neurons of rat hippocampal slices. *J Physiol (Lond)* 458: 261–287, 1992.

CONTI F AND MANZONI T. The neurotransmitters and postsynaptic actions of callosally projecting neurons. *Behav Brain Res* 64: 37–53, 1994.

CULL-CANDY SG, HOWE JR, AND OGDEN DC. Noise and single channels activated by excitatory amino acids in rat cerebellar granule neurons. *J Physiol (Lond)* 400: 189–222, 1988.

DOBRUNZ LE AND STEVENS CF. Heterogeneity of release probability, facilitation, and depression at central synapses. *Neuron* 18: 995–1008, 1997.

DOUGLAS RJ, KOCH C, MAHOWALD M, MARTIN KAC, AND SUAREZ HH. Recurrent excitation in neocortical circuits. *Science* 269: 981–985, 1995.

FELDMEYER D, EGGER V, LUBKE J, AND SAKMANN B. Reliable synaptic connections between pairs of excitatory layer 4 neurones within a single 'barrel' of developing rat somatosensory cortex. *J Physiol (Lond)* 521: 169–190, 1999.

FLEIDERVISH IA, BINSHTOK AM, AND GUTNICK MJ. Functionally distinct NMDA receptors mediate horizontal connectivity within layer 4 of mouse barrel cortex. *Neuron* 21: 1055–1065, 1998.

GAZZANIGA MS, RISSE GL, SPRINGER SP, CLARK DE, AND WILSON DH. Psychologic and neurologic consequences of partial and complete cerebral commissurotomy. *Neurology* 25: 10–15, 1975.

GEIGER JR, LUBKE J, ROTH A, FROTSCHER M, AND JONAS P. Submillisecond AMPA receptor–mediated signaling at a principal neuron-interneuron synapse. *Neuron* 18: 1009–1023, 1997.

GEIGER JR, MELCHER T, KOH DS, SAKMANN B, SEEBURG PH, JONAS P, AND MONYER H. Relative abundance of subunit mRNAs determines gating and Ca^{2+} permeability of AMPA receptors in principal neurons and interneurons in rat CNS. *Neuron* 15: 193–204, 1995.

GIL Z AND AMITAI Y. Adult thalamocortical transmission involves both NMDA and non-NMDA receptors. *J Neurophysiol* 76: 2547–2554, 1996.

GIL Z, CONNORS BW, AND AMITAI Y. Differential regulation of neocortical synapses by neuromodulators and activity. *Neuron* 19: 679–686, 1997.

GIL Z, CONNORS BW, AND AMITAI Y. Efficacy of thalamocortical and intracortical synaptic connections: quanta, innervation, and reliability. *Neuron* 23: 385–397, 1999.

GLOBUS A AND SCHEIBEL AB. Synaptic loci on parietal cortical neurons; terminations of corpus callosum fibers. *Science* 156: 1127–1129, 1967.

GODA Y AND STEVENS CF. Readily releasable pool size changes associated with long-term depression. *Proc Natl Acad Sci USA* 95: 1283–1288, 1998.

HAMILL OP, MARTY A, NEHER E, SAKMANN B, AND SIGWORTH FJ. Improved patch-clamp techniques for high-resolution current recording from cells and cell-free membrane patches. *Pflügers Arch* 391: 85–100, 1981.

HAUSSER M AND ROTH A. Estimating the time course of the excitatory synaptic conductance in neocortical pyramidal cells using a novel voltage jump method. *J Neurosci* 17: 7606–7625, 1997.

HESTRIN S. Developmental regulation of NMDA receptor–mediated synaptic currents at a central synapse. *Nature* 357: 686–689, 1992.

HESTRIN S. Different glutamate receptor channels mediate fast excitatory synaptic currents in inhibitory and excitatory cortical neurons. *Neuron* 11: 1083–1091, 1997.

HESTRIN S, NICOLL RA, PERKEL DJ, AND SAH P. Analysis of excitatory synaptic action in pyramidal cells using whole-cell recording from rat hippocampal slices. *J Physiol (Lond)* 422: 203–225, 1990.

INNOCENTI GM. *Cerebral Cortex.* New York: Plenum, 1986, p. 291–335.

IVY GO AND KILLACKEY HP. The ontogeny of the distribution of callosal projection neurons in the rat parietal cortex. *J Comp Neurol* 195: 367–389, 1981.

JACOBSON S. Intralaminar, interlaminar, callosal and thalamocortical connections in frontal and parietal areas of the albino rat cerebral cortex. *J Comp Neurol* 124: 131–146, 1965.

JACOBSON S AND TROJANOWSKI JQ. The cells of origin of the corpus callosum in rat, cat and rhesus monkey. *Brain Res* 74: 149–155, 1974.

JOHNSON RR, JIANG X, AND BURKHALTER A. Regional and laminar differences in synaptic localization of NMDA receptor subunit NR1 splice variants in rat visual cortex and hippocampus. *J Comp Neurol* 368: 335–355, 1996.

JONAS P AND BURNASHEV N. Molecular mechanisms controlling calcium entry through AMPA-type glutamate receptor channels. *Neuron* 15: 987–990, 1995.

JONAS P, RACCA C, SAKMANN B, SEEBURG PH, AND MONYER H. Differences in calcium permeability of AMPA-type glutamate receptor channels in neocortical neurons caused by differential GluR-B subunit expression. *Neuron* 12: 1281–1289, 1994.

JONAS P AND SAKMANN B. Glutamate receptor channels in isolated patches from CA1 and CA3 pyramidal cells of rat hippocampal slices. *J Physiol (Lond)* 455: 143–171, 1992.

KAWAGUCHI Y. Receptor subtypes involved in callosally-induced postsynaptic potentials in rat frontal cortex in vitro. *Exp Brain Res* 88: 33–40, 1992.

KELLER BU, KONNERTH A, AND YAARI Y. Patch clamp analysis of excitatory synaptic currents in granule cells of rat hippocampus. *J Physiol (Lond)* 435: 275–293, 1991.

KIDD FL AND ISAAC TR. Developmental and activity-dependent regulation of kainate receptors at thalamocortical synapses. *Nature* 400: 569–573, 1999.

KISVARDAY ZF, MARTIN KAC, FREUND TF, MAGLOCZKY Z, WHITTERIDGE D, AND SOMOGYI P. Synaptic targets of HRP-filled layer III pyramidal cells in the cat striate cortex. *Exp Brain Res* 64: 541–552, 1986.

KUMAR SS, BACCI A, KHARAZIA V, AND HUGUENARD JR. Influx of calcium through synaptic AMPA receptors in rat pyramidal neurons is developmentally regulated (Abstract). *Soc Neurosci.* In press.

KUMAR SS AND HUGUENARD JR. Functional properties of cortico-cortical synapses in the callosal model. *Epilepsia* 40: 10–11, 1999.

LAMBERT NA AND WILSON AW. Heterogeneity in presynaptic regulation of GABA release from hippocampal inhibitory neurons. *Neuron* 11: 1057–1067, 1993.

LERMA J, MORALES M, IBARZ JM, AND SOMOHANO F. Rectification properties and Ca^{2+} permeability of glutamate receptor channels in hippocampal cells. *Eur J Neurosci* 6: 1080–1088, 1994.

LEWIS CA. Ion-concentration dependence of the reversal potential and single channel conductance of ion channels at the frog neuromuscular junction. *J Physiol (Lond)* 286: 417–445, 1979.

LUHMANN HJ AND PRINCE DA. Transient expression of polysynaptic NMDA receptor-mediated activity during neocortical development. *Neurosci Lett* 111: 109–115, 1990.

MARKRAM H, LUBKE J, FROTSCHER M, ROTH A, AND SAKMANN B. Physiology and anatomy of synaptic connections between thick tufted pyramidal neurones in the developing neocortex. *J Physiol (Lond)* 500: 409–440, 1997.

MAYER ML AND WESTBROOK GL. Permeation and block of *N*-methyl-D-aspartic acid receptor channels by divalent cations in mouse cultured central neurones. *J Physiol (Lond)* 394: 501–527, 1987.

MCBAIN CJ AND DINGLEDINE R. Heterogeneity of synaptic glutamate receptors on CA3 stratum radiatum interneurones of rat hippocampus. *J Physiol (Lond)* 462: 373–392, 1993.

MCGUIRE BA, HORNUNG JP, GILBERT CD, AND WIESEL TN. Patterns of synaptic input to layer 4 of cat striate cortex. *J Neurosci* 4: 3021–3033, 1984.

MOSHE SL, ALBALA BJ, ACKERMANN RF, AND ENGEL J JR. Increased seizure susceptibility of the immature brain. *Dev Brain Res* 7: 81–85, 1983.

OLAVARRIA J AND VAN SLUYTERS RC. Axons from restricted regions of the cortex pass through restricted portions of the corpus callosum in adult and neonatal rats. *Brain Res* 390: 309–313, 1986.

PANDYA DN AND SELTZER B. *Two Hemispheres—One Brain: Functions of the Corpus Callosum.* New York: Liss, 1986, p. 47–73.

PAXINOS G AND WATSON C. *The Rat Brain in Stereotaxic Coordinates* (2nd ed.). San Diego, CA: Academic, 1986.

PELLETIER MR AND HABLITZ JJ. Altered desensitization produces enhancement of EPSPs in neocortical neurons. *J Neurophysiol* 72: 1032–1036, 1994.

REEVES AG AND O'LEARY PM. *Epilepsy and the Corpus Callosum*. New York: Plenum, 1985, p. 269–280.

REYES A AND SAKMANN B. Developmental switch in the short-term modification of unitary EPSPs evoked in layer 2/3 and layer 5 pyramidal neurons of rat neocortex. *J Neurosci* 19: 3827–3835, 1999.

ROZOV A AND BURNASHEV N. Polyamine-dependent facilitation of postsynaptic AMPA receptors counteracts paired-pulse depression. *Nature* 401: 594–598, 1999.

SUTOR B AND LUHMANN HJ. Involvement of GABA(B) receptors in convulsant-induced epileptiform activity in rat neocortex in vitro. *Eur J Neurosci* 10: 3417–3427, 1998.

SWANN JW, SMITH KL, BRADY RJ, AND PIERSON MG. *Epilepsy: Models, Mechanisms, and Concepts*. Cambridge, UK: Cambridge Univ. Press, 1993.

THOMSON AM. A magnesium-sensitive post-synaptic potential in rat cerebral cortex resembles neuronal responses to *N*-methylaspartate. *J Physiol (Lond)* 370: 531–549, 1986.

THOMSON AM. Facilitation, augmentation and potentiation at central synapses. *Trends Neurosci* 23: 305–312, 2000.

THOMSON AM, DEUCHARS J, AND WEST DC. Large, deep layer pyramid-pyramid single axon EPSPs in slices of rat motor cortex display paired pulse and frequency-dependent depression, mediated presynaptically and self-facilitation, mediated postsynaptically. *J Neurophysiol* 70: 2354–2369, 1993.

THOMSON AM AND WEST DC. Fluctuations in pyramid-pyramid excitatory postsynaptic potentials modified by presynaptic firing pattern and postsynaptic membrane potential using paired intracellular recordings in rat neocortex. *Neuroscience* 54: 329–346, 1993.

TRAYNELIS SF, SILVER RA, AND CULL-CANDY SG. Estimated conductance of glutamate receptor channels activated during EPSCs at the cerebellar mossy fiber-granule cell synapse. *Neuron* 11: 279–289, 1993.

VOGT BA AND GORMAN ALF. Responses of cortical neurons to stimulation of corpus callosum in vitro. *J Neurophysiol* 48: 1257–1273, 1982.

WASHBURN MS, NUMBERGER M, ZHANG S, AND DINGLEDINE R. Differential dependence on GluR2 expression of three characteristic features of AMPA receptors. *J Neurosci* 17: 9393–9406, 1997.

WILSON DH, CULVER C, WADDINGTON M, AND GAZZANIGA M. Disconnection of the cerebral hemispheres: an alternative to hemispherectomy for control of intractable seizures. *Neurology* 25: 1149–1153, 1975.

WISE SP AND JONES EG. The organization and postnatal development of the commissural projection of the rat somatic sensory cortex. *J Comp Neurol* 168: 313–344, 1976.

YIN HZ, SENSI SL, CARRIEDO SG, AND WEISS JH. Dendritic localization of Ca^{2+} permeable AMPA/Kainate channels in hippocampal pyramidal neurons. *J Comp Neurol* 409: 250–260, 1999.

ZHOU F-M AND HABLITZ JJ. Rapid kinetics and inward rectification of miniature EPSCs in layer I neurons of rat neocortex. *J Neurophysiol* 77: 2416–2426, 1997.